Available online at www.sciencedirect.com
SCIENCE DIRECT®
PERGAMON
Polyhedron 22 (2003) 2545–2556
POLYHEDRON
www.elsevier.com/locate/poly

Magnetic properties of complex d^1 and d^5 ions: crystal field model and Jahn–Teller effect

Kim R. Dunbar [a,*], Eric J. Schelter [a], Boris S. Tsukerblat [b,*], Sergei M. Ostrovsky [c], Vadim Yu. Mirovitsky [c], Andrew V. Palii [c]

[a] Department of Chemistry, Texas A&M University, College Station, TX 77842-3012, USA
[b] Department of Chemistry, Ben-Gurion University of the Negev, P.O. Box 84105, Beer-Sheva 84105, Israel
[c] Institute of Applied Physics, Academy of Sciences of Moldova, Academy str. 5, Kishinev MD-2028, Moldova

Received 20 November 2002; accepted 18 February 2003

Abstract

In this paper, the low lying levels of d^1 and low-spin d^5 metal complexes possessing ground $^2T_2$ term are considered. Strong spin–orbital interactions is taken into account along with the axial (trigonal or tetragonal) component of the crystal field. In the framework of the semi-classic adiabatic approximation, vibronic Jahn–Teller and pseudo Jahn–Teller interactions acting within the ground manifold are also considered. The influence of the low-symmetry crystal fields, covalence reduction factor, spin–orbital and Jahn–Teller interactions on the anisotropy of g-factors, temperature independent paramagnetic contributions, and magnetic susceptibility is elucidated.

Keywords: d^1 and d^5 metal complexes; Magnetic properties; Jahn–Teller effect

1. Introduction

Coordination complexes of paramagnetic metal ions of the second and third transition series have attracted considerable interest due to strong spin–orbital interactions giving rise to a significant magnetic anisotropy. In the course of our studies of the two compounds $[Et_4N][Re(triphos)(CN)_3]$ and $[Re(triphos)(CH_3CN)_3][BF_4]_2$ [1], in which Re(II) ions occupy the sites with a strong cubic crystal field and a significant trigonal component, observation of unusual temperature dependent magnetic behavior has prompted us to launch an in-depth analysis of the magnetism of this ion. These complexes exhibit anomalously large temperature independent paramagnetism (TIP) ($1.363\cdot10^{-3}$ $cm^3\,mol^{-1}$ and $1.796\cdot10^{-3}$ $cm^3\,mol^{-1}$, respectively) that can be related to a set of low lying excited states. The interplay between a low-symmetry crystal field and spin–orbital and vibronic interactions in the complexes gives rise to the important low-lying excited states. As the cubic crystal field for 5d metal ions is always strong, the d^5 electronic configuration yields a low-spin ground state term, $^2T_2(t_2^4)$, that is split by the spin–orbital interaction and a trigonal crystal field. The ground state term of the same symmetry ($^2T_2(t_2)$) appears in the case of d^1 ions, but the sign of the spin–orbital interaction is opposite (positive for d^1 and negative for d^5). This formal similarity allows for the consideration of both electronic configurations in the same framework. Previous studies of orbital triplets in a crystal field have focused mainly on the calculation of the EPR parameters [2–5]. In the present study T–P isomorphism [3] is used to describe the magnetic properties of d^1 and d^5 systems.

Vibronic Jahn–Teller (JT) interactions are important for the interpretation of the magnetic and spectroscopic properties of transition metal complexes [6–8]. The special importance of the JT interaction to magnetic behavior has been noted [9], and has led to the discovery of the giant second-order Zeeman effect. This effect was shown to arise from the set of closely spaced hybrid

* Corresponding authors. Tel.: +1-979-845-5235; fax: +1-979-845-7177.
E-mail addresses: dunbar@mail.chem.tamu.edu (K.R. Dunbar), tsuker@bgumail.bgu.ac.il (B. Tsukerblat), sm_ostrovsky@yahoo.com (S.M. Ostrovsky).

0277-5387/03/$ - see front matter © 2003 Elsevier Science Ltd. All rights reserved.
doi:10.1016/S0277-5387(03)00294-8

electron-vibrational levels. The JT interaction for the extended 5d electronic shells is expected to be strong, and must be taken into account along with the spin–orbital interaction in order to understand the magnetism of these systems. This leads to a combined JT and pseudo-JT problem. Using a semi-classical adiabatic approach [10] we have elucidated the main manifestation of the JT interaction in the magnetic properties of the systems under consideration.

2. The model

Ions of the type d^1 and d^5 in a perfect octahedral surrounding (O_h) as well as in an axially distorted system are considered. Axial distortions are assumed to arise from the mixed ligand sets or from deviation of the local surroundings of the metal ion from an octahedral one. Either of the conditions gives rise to a trigonal or a tetragonal component of the crystal field. The model takes into account the following relevant interactions defining the magnetic properties of the complexes: (1) a strong cubic crystal field that splits the ^{2}D term of a free d^1 ion into the orbital triplet $^2T_{2g}$ (ground state) and the doublet ^2E_g (hereafter symbol of the parity will be omitted) or the triplet ground state $^2T_2(t_2^4)$ in the case of the d^5 ion; (2) spin–orbit coupling that splits the $^2T_2$-term into the doublet Γ_6 and the quadruplet Γ_8; (3) tetragonal or trigonal components of the crystal field; (4) vibronic coupling in the orbital triplet with the tetragonal (e) and trigonal (t_2) modes that lead to a combined JT and pseudo JT vibronic problem $T_2 \otimes (e + t_2 + SO)$. Initially the study of the JT problem will be limited to the case of a cubic system (the combined effect of low-symmetry fields and the JT interaction will be considered elsewhere). The adiabatic approximation, shown to provide good accuracy in the calculation of the magnetic susceptibility for JT type vibronic systems for a wide range of parameters [10], will be employed. This approximation allows us to gain a descriptive comprehension of the physical role of the JT interaction. The full Hamiltonian of the system in the adiabatic approximation can be written as follows:

$$\begin{aligned} H = {} & H_{SO} + V_{tetr} + V_{trig} + H_Z + \tfrac{1}{2}\,\omega_E(q_u^2 + q_v^2)I \\ & + \tfrac{1}{2}\,\omega_{r_2}(q_\xi^2 + q_\eta^2 + q_\zeta^2)I + \upsilon_E(q_u O_u + q_v O_v) \\ & + \upsilon_{T_2}(q_\xi O_\xi + q_\eta O_\eta + q_\zeta O_\zeta), \end{aligned} \tag{1}$$

The Hamiltonian of the electronic subsystem includes spin–orbit coupling (H_{SO}), low-symmetry crystal fields ($V_{tetr} + V_{trig}$) and a Zeeman interaction (H_Z). The vibronic part of the Hamiltonian includes the energy of free vibrations associated with the tetragonal (T_2) and trigonal (E) JT modes, and the vibronic coupling with these modes (coupling constants υ_E and υ_{T_2}). The dimensionless normal coordinates of the tetragonal vibrations are denoted as q_u, q_v (basis $u \propto 3z^2 - r^2$, $v \propto x^2 - y^2$) and those for the trigonal vibrations are q_ξ, q_η, q_ζ ($\xi \propto xz$, $\eta \propto xz$, $\zeta \propto xy$), while ω_E and ω_{T_2} are the frequencies of these vibrations. In Eq. (1), I is the unit matrix and the matrices $O_{\Gamma\gamma}$ (active modes $\Gamma = E$, T_2) defined in the cubic T_2-basis (ξ, η, ζ) are the following:

$$\begin{aligned} O_{Eu} &= \begin{pmatrix} -1/2 & 0 & 0 \\ 0 & -1/2 & 0 \\ 0 & 0 & 1 \end{pmatrix}, \\ O_{Ev} &= \begin{pmatrix} \sqrt{3}/2 & 0 & 0 \\ 0 & -\sqrt{3}/2 & 0 \\ 0 & 0 & 0 \end{pmatrix} \\ O_{T_2\xi} &= \begin{pmatrix} 0 & 0 & 0 \\ 0 & 0 & 1 \\ 0 & 1 & 0 \end{pmatrix}, \quad O_{T_2\eta} = \begin{pmatrix} 0 & 0 & 1 \\ 0 & 0 & 0 \\ 1 & 0 & 0 \end{pmatrix}, \quad O_{T_2\zeta} \\ &= \begin{pmatrix} 0 & 1 & 0 \\ 1 & 0 & 0 \\ 0 & 0 & 0 \end{pmatrix}. \end{aligned} \tag{2}$$

Eq. (1) uses a short notation for the matrices $O_{\Gamma\gamma}{:}O_{\Gamma\gamma} \equiv O_\gamma$. In the framework of the adopted semi-classic adiabatic approximation the kinetic energy of the nuclear motion is omitted.

3. Matrix representation of the main interactions

T–P isomorphism is used to allow for the consideration of the orbital triplet T_2 as a state possessing fictious orbital angular momentum $L = 1$, noting that the matrix elements of the angular momentum operator $\hat{L}$ within T_2 and P bases are of the opposite signs, $\hat{L}(T_2) = -\hat{L}(P)$ [3]. As was shown recently [11], this approach provides an efficient computational tool and yields clear insight on the magnetic anisotropy of the system due to orbital contributions. Within the T–P formalism the spin–orbit and Zeeman terms can be expressed as:

$$H_{SO} = -\kappa\lambda LS, \quad H_Z = \beta(g_e S - \kappa L)H, \tag{3}$$

The operators in Eq. (3) act within the ground state manifold possessing $S = {}^1/_2$ and $L = 1$ (κ is the orbital reduction factor, g_e is the electronic g-factor). The tetragonal and trigonal components of the crystal field are defined as the irreducible tensors of O_h that become the scalar operators in the tetragonal or trigonal point groups (D_{3d} or D_{4h}):

$$\begin{aligned} V_{tetr} &= -\Delta_{tetr} O_{Eu}, \quad V_{trig} \\ &= -\tfrac{1}{2}\,\Delta_{trig}(O_{T_2\xi} + O_{T_2\eta} + O_{T_2\zeta}) \end{aligned} \tag{4}$$

In Eq. (4) the values Δ_{tetr} and Δ_{trig} are the parameters of the low symmetry crystal fields. Axial crystal field along the C_4 or C_3 axis splits T_2 into an orbital singlet or

a doublet in D_{4h} or D_{3d}. The parameters Δ_{tetr} and Δ_{trig} are defined in such a way that when positive, the ground state in the axial field is the orbital singlet.

To take advantage of the pseudoangular momentum representation, the technique of the irreducible tensor operators shall be employed [11]. One can easily establish the following relations between the matrices $O_{\Gamma\gamma}$ and the orbital angular momentum operators:

$$O_{Eu} = 1 - \tfrac{3}{2} L_Z^2, \quad O_{Ev} = -\tfrac{\sqrt{3}}{2}(L_X^2 - L_Y^2), \tag{5}$$
$$O_{T_2\xi} = -\tfrac{1}{\sqrt{2}}(L_Y L_Z + L_Z L_Y), \quad O_{T_2\eta} = -\tfrac{1}{\sqrt{2}}(L_X L_Z + L_Z L_X),$$
$$O_{T_2\zeta} = -\tfrac{1}{\sqrt{2}}(L_X L_Y + L_Y L_X).$$

The operators L_X, L_Y and L_Z can be expressed in terms of the components of the first rank spherical irreducible tensor $L_{1q}(q = 0, \pm 1)$:

$$L_X = \tfrac{1}{\sqrt{2}}(L_{1-1} - L_{11}), \quad L_Y = \tfrac{1}{\sqrt{2}}(L_{1-1} + L_{11}),$$
$$L_Z = L_{10}, \tag{6}$$

and the same relationships can be applied for spin operators. Using the Clebsch–Gordan decomposition [12], the bilinear forms of the orbital angular momentum operators in Eq. (6) can be expressed in terms of the irreducible tensor products:

$$L_{1q_1} L_{1q_2} = \sum_{kq} \{L_1 \otimes L_1\}_{kq} C^{kq}_{1q_1\ 1q_2} \tag{7}$$

Here $\{L_1 \otimes L_1\}_{kq}$ is the complex irreducible tensor of the rank k composed of the angular momentum operators ($q = -k, -k+1 \ldots$ k), and $C^{kq}_{1q1\ 1q2}$ are the Clebsch–Gordan (Wigner) coefficients. All matrices $O_{\Gamma\gamma}$ can now be expressed in terms of the complex irreducible tensors $T_{kq}(L) = \{L_1 \otimes L_1\}_{kq}$ acting in orbital space:

$$O_{Eu} = -\sqrt{\tfrac{3}{2}}\, T_{20}(L), \quad O_{Ev} = -\tfrac{\sqrt{3}}{2}[T_{22}(L) + T_{2-2}(L)], \tag{8}$$
$$O_{T_2\xi} = -\tfrac{i}{\sqrt{2}}[T_{21}(L) + T_{2-1}(L)],$$
$$O_{T_2\eta} = \tfrac{1}{\sqrt{2}}[T_{21}(L) - T_{2-1}(L)],$$
$$O_{T_2\zeta} = -\tfrac{i}{\sqrt{2}}[T_{22}(L) - T_{2-2}(L)].$$

These relationships allow for the evaluation of the matrix elements of all interactions involved using the irreducible tensor operator technique and exploiting the results in the study of magnetically coupled systems. The matrix can be built with either coupled or uncoupled bases. It is convenient to choose the basis in such a way that spin–orbit coupling would become diagonal, that is, to take a basis wherein the orbital angular momentum and spin are coupled $|LSJM_J\rangle \equiv |1^1/_2 JM_J\rangle$, and where the total angular momentum takes the values $J = \frac{1}{2}$ (Kramer's doublet Γ_6) and $J = \frac{3}{2}$ (quadruplet Γ_8). Keeping in mind the application of the present theory to the more complicated cases (Ex: Co(II) ions or exchange-coupled systems), more general formulae for the arbitrary values of S are given. The spin–orbit interaction is represented by the diagonal matrix:

$$\langle 1SJ'M'_J|H_{SO}|1SJM_J\rangle = -\tfrac{1}{2}\kappa\lambda[J(J+1) - S(S+1) - 2]\delta_{JJ'}, \quad \delta_{M_JM'_J}. \tag{9}$$

Then, with the aid of Ref. [12] the following expression for the matrix elements of the vibronic interaction is obtained:

$$\begin{aligned}\langle 1SJ'M'_J|H_{vib}|1SJM_J\rangle &= (-1)^{1+S+J}\sqrt{5(2J+1)}\begin{Bmatrix}1 & 2 & 1\\ J' & S & J\end{Bmatrix}\\ &\times\{-v_E\tfrac{\sqrt{3}}{2}[q_u\sqrt{2}\,C^{J'M'_J}_{JM_J\ 20} + q_v(C^{J'M'_J}_{JM_J\ 22} + C^{J'M'_J}_{JM_J\ 2-2})]\\ &+\tfrac{1}{\sqrt{2}}v_{T_2}[-iq_\xi(C^{J'M'_J}_{JM_J\ 21} + C^{J'M'_J}_{JM_J\ 2-1})\\ &+q_\eta(C^{J'M'_J}_{JM_J\ 21} - C^{J'M'_J}_{JM_J\ 2-1})\\ &+iq_\zeta(C^{J'M'_J}_{JM_J\ 22} - C^{J'M_J}_{JM_J\ 2-2})]\},\end{aligned} \tag{10}$$

where $\begin{Bmatrix}\cdots\\ \cdots\end{Bmatrix}$ are the 6j-symbols [12]. For the matrix elements of the Zeeman interaction:

$$\begin{aligned}\langle 1SJ'M'_J|H_Z|1SJM_J\rangle &= \sqrt{(2J+1)}(-1)^{J+S}\begin{Bmatrix}1 & 1 & 1\\ J' & S & J\end{Bmatrix}\\ &\times\beta[g_e\sqrt{S(S+1)(2S+1)} + \kappa\sqrt{6}]\\ &\times(C^{J'M'_J}_{JM_J\ 10}H_{10} - C^{J'M'_J}_{JM_J\ 11}H_{1-1} - C^{J'M'_J}_{JM_J\ 1-1}H_{11})\end{aligned} \tag{11}$$

is obtained, where $H_{10} = H_Z$, $H_{1\pm1} = \mp\frac{1}{\sqrt{2}}(H_X \pm iH_Y)$ are the cyclic components of the magnetic field. Particular direction of the magnetic field can be selected by means of an appropriate choice of the corresponding terms in Eq. (11). For the matrix elements of the tetragonal and trigonal crystal field operators we find:

$$\begin{aligned}\langle 1SJ'M'_J|V_{tetr} + V_{trig}|1SJM_J\rangle &= (-1)^{1+S+J}\sqrt{5(2J+1)}\begin{Bmatrix}1 & 2 & 1\\ J' & S & J\end{Bmatrix}\\ &\times\{\sqrt{\tfrac{3}{2}}\Delta_{tetr}C^{J'M'_J}_{JM_J\ 20}\\ &+\tfrac{1}{2\sqrt{2}}\Delta_{trig}[(i-1)C^{J'M'_J}_{JM_J\ 21} + (i+1)C^{J'M'_J}_{JM_J\ 2-1}\\ &-i(C^{J'M'_J}_{JM_J\ 22} - C^{J'M'_J}_{JM_J\ 2-2})]\}.\end{aligned} \tag{12}$$

In the following sections the static (crystal field) problem and the role of the JT and pseudo JT coupling will be considered.

4. Static crystal field consideration, general expressions

The spin–orbit coupling parameter is positive for d^1-ions and negative for the low-spin d^5-ions, so that for d^1 quadruplet Γ_8 is the ground state, and the low-spin d^5 ground state is the Kramers doublet Γ_6. The energy levels are the following:

$$E\left(\frac{1}{2}\right) = k\lambda, \quad E\left(\frac{3}{2}\right) = -\frac{k\lambda}{2}, \tag{13}$$

so the energy gap between the doublet and quadruplet is $3\kappa|\lambda|/2$. When both spin–orbit coupling and the axial (trigonal or tetragonal) field act together, the states $\|M_J = \frac{1}{2}\rangle$ belonging to $J = \frac{1}{2}$ and $J = \frac{3}{2}$ (Γ_7 and Γ_8 in O) are mixed due to axial symmetry of the full Hamiltonian so that only M_J remains a good quantum number. The quantization axis for the full angular momentum in the case of the tetragonal distortion is C_4 and for the trigonal distortion this axis is C_3. Hereafter the results are discussed assuming the system is trigonally distorted ($\Delta \equiv \Delta_{trig}$). The results for the case of the tetragonal field are formally the same. The energy levels $E(|M_J|)$ are found as:

$$E_{\pm}(\tfrac{1}{2}) = \tfrac{1}{4}[-\Delta + \lambda k \pm \sqrt{(\Delta + 3\lambda k)^2 + 8\Delta^2}], \quad E\left(\frac{3}{2}\right) = \frac{\Delta}{2} - \frac{\lambda k}{2}, \tag{14}$$

The minus sign in $E_{\pm}(\frac{1}{2})$ corresponds to the sublevel originating from the $J = \frac{3}{2}$ state that is mixed with the $J = \frac{1}{2}$, $M_J = \frac{1}{2}$ state. Fig. 1a shows the energy levels of the d^1 system as a function of Δ providing $\lambda k = 2000\ \mathrm{cm}^{-1}$. A positive trigonal field stabilizes the Kramers doublet $E_-(\frac{1}{2})(M_J = \pm\frac{1}{2},\ J = \frac{1}{2}, \frac{3}{2})$, in the limit of a strong trigonal field, the ground state being $^2A_1$ in conformity with the definition of the crystal field operator, Eq. (4). Provided that $\Delta < 0$ the ground state corresponds to $J = \frac{3}{2}$, $M_J = \pm\frac{3}{2}$. In this case, in the limit of the strong field, two low-lying levels $E(\frac{3}{2})$, $E_-(\frac{1}{2})$ are parallel and can be attributed to the first order spin–orbital splitting of the trigonal ^2E term in D_{3d} (complex conjugated double valued representations $\Gamma_5+\Gamma_6$ with the basis $M_J = \pm\frac{3}{2}$ and Γ_4-basis $M_J = \pm\frac{1}{2}$). Only the $\hat{L}_z$ component is operative within the orbital trigonal basis E, so that spin–orbit coupling becomes axial ($-k\lambda \underline{L}_z S_z$) and one easily finds that the spin–orbit splitting is $k\lambda$. This value is reduced by the trigonal crystal field with respect to its initial value ($3k\lambda/2$) in a cubic $^2T_2$ term. For d^5 ions, spin–orbit coupling is negative and the order of the levels is reversed as shown in Fig. 1b.

Some details of the calculations of the magnetic characteristics of the d^1 ion when the quadruplet Γ_8 proves to be the ground state are given. For evaluation of the first and second order coefficients in the Van Vleck equation [13], the eigen-vectors $\Phi_{\pm}(M_J = \pm\frac{1}{2})$ of the 2×2-matrix for the mixing of two $|M_J| = \frac{1}{2}$ ($J = \frac{1}{2}, \frac{3}{2}$) states are:

$$\begin{aligned}\Phi_+(\pm\tfrac{1}{2}) &= \cos\theta \exp(i\alpha_{\pm})|\tfrac{1}{2}, \pm\tfrac{1}{2}\rangle \\ &\quad + \sin\theta \exp(-i\alpha_{\pm})|\tfrac{3}{2}, \pm\tfrac{1}{2}\rangle \\ \Phi_-(\pm\tfrac{1}{2}) &= -\sin\theta \exp(i\alpha_{\pm})|\tfrac{1}{2}, \pm\tfrac{1}{2}\rangle \\ &\quad + \cos\theta \exp(-i\alpha_{\pm})|\tfrac{3}{2}, \pm\tfrac{1}{2}\rangle\end{aligned} \tag{15}$$

where the angle θ is defined as:

$$\tan h\theta = \frac{2\sqrt{2}|\Delta|}{\Delta + 3\lambda k + \sqrt{(\Delta + 3\lambda k)^2 + 8\Delta^2}},$$

$$\exp(2i\alpha_{\pm}) = \pm\frac{\Delta}{|\Delta|}.$$

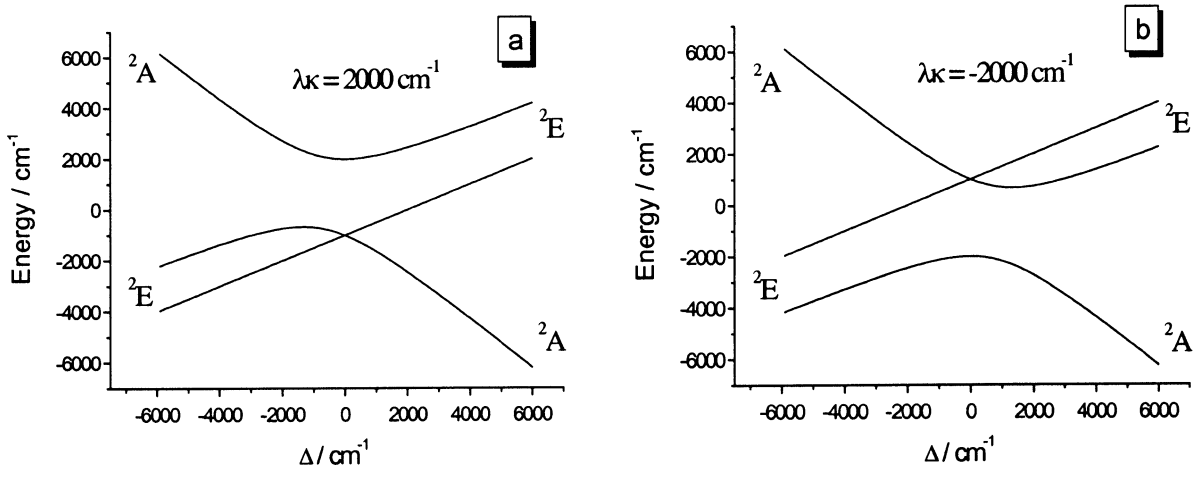

Fig. 1. Splittings of the $^2T_2$ term for d^1 (a) and d^5 (b) ions under the joint action of spin–orbit interactions and axial (trigonal or tetragonal) crystal fields.

Two separate, qualitatively different cases, namely positive and negative trigonal crystal fields, are now considered. The combined action of spin–orbital interaction and trigonal crystal field is expected to produce magnetic anisotropy, so two main directions of the magnetic field, namely, $H||C_3$ axis and $H\perp C_3$ ($H\|$X) (parallel and perpendicular fields) will be considered.

(1) $\Delta>0$. Using the wavefunctions for the ground state $\Phi_-(\pm\frac{1}{2})$ one can find the first order Zeeman splitting that gives the following expressions for the g-factors:

$$g_{zz}\equiv g_{\|}=-k+\frac{1}{3}(k+g_e)[\cos 2\theta+2\sqrt{2}\sin 2\theta] \tag{16}$$

$$g_{xx}\equiv g_{\perp}=\frac{1}{2}\,g_e+\frac{1}{6}(g_e-8k)\cos 2\theta+\frac{\sqrt{2}}{3}(g_e+k)\sin 2\theta$$

Both g-factors vanish when $k=1$ ($g_e=2$) and $\Delta=0$. This reflects the property of the cubic quadruplet $\Gamma_8(J=\frac{3}{2})$ arising from $^2T_2$ that does not exhibit first order magnetic splitting. This important property of $\Gamma_8(^2T_2)$ can be easily rationalized. In fact, providing $k=1$, the matrix element of the Zeeman interaction vanishes due to opposite signs of L in P and T_2 ('negative' orbital angular momentum), in the last case spin and orbital magnetic contributions are cancelled. This consideration shows that the non-vanishing g-values are determined by two factors, namely the degree of mixing of two $J=\frac{1}{2}$ doublets via the trigonal field and by the factor of covalence (k). The covalence effect decreases the orbital magnetic moment so that the condition for compensation of the orbital and spin contributions is broken.

Using the Van Vleck equation [13] and Eqs. (15) and (16) one can find the following expressions for the principal magnetic susceptibilities for the case of $\Delta>0$ related to the ground state:

$$\chi_{\|}=\frac{N\beta^2}{4k_BT}\,g_{\|}^2+\frac{2N\beta^2(k+g_e)^2[\sin 2\theta-2\sqrt{2}\cos 2\theta]^2}{18\sqrt{(\Delta+3\lambda k)^2+8\Delta^2}} \tag{17}$$

$$\chi_{\perp}=\frac{N\beta^2}{4k_BT}\,g_{\perp}^2+2N\beta^2\left\{\frac{[(k+g_e)\cos 2\theta-(1/2\sqrt{2})(g_e-8k)\sin 2\theta]^2}{\sqrt{3}\sqrt{(\Delta+3\lambda k)^2+8\Delta^2}}\right\}+\frac{[32(k+g_e)\sin\theta-16\sqrt{2}(g_e-2k)\cos\theta]^2}{3[3\Delta-3k\lambda+\sqrt{(\Delta+3\lambda k)^2+8\Delta^2}]}$$

In Eq. (17) the first terms are the paramagnetic contributions (principal g-factors are given by Eq. (16)), and the second terms represent the TIP contribution.

(2) $\Delta<0$. As in the previous case, only the contributions from the ground state are taken into account. As was already mentioned, the $|\frac{3}{2},\pm\frac{3}{2}\rangle$ states remain unmixed in a parallel field, so that for this ground state the TIP vanishes. Contrary to this, the first order magnetic splitting obviously disappears in the perpendicular field. The expressions for the principal components of the magnetic susceptibilities are found as:

It is remarkable that, in the case of negative trigonal field, $\chi_{\|}$ does not contain TIP and involves only a paramagnetic component, whereas TIP contributes only to $\chi_{\perp}$. For the aforementioned reasons $\chi_{\|}$ vanishes when $k=1$ and proves to be independent of the strength of the trigonal field. For the ground state in the case under consideration, the g-factors take on the values $g_{\|}=g_e-2k$ and $g_{\perp}=0$, so that the magnetic moment and susceptibility for this ground state are fully anisotropic.

$$\chi_{\|}=\frac{N\beta^2}{4k_BT}(g_e-2k)^2 \tag{18}$$

$$\chi_{\perp}=\frac{N\beta^2}{3}\left[\frac{3(g_e^2+2k^2)-(g_e^2-2k^2+8g_ek)\cos 2\theta+2\sqrt{2}(g_e^2-2k^2+g_ek)\sin 2\theta}{3\lambda k-3\Delta-\sqrt{(\Delta+3\lambda k)^2+8\Delta^2}}\right]+\left[\frac{3(g_e^2+2k^2)+(g_e^2+2k^2-8g_ek)\cos 2\theta-2\sqrt{2}(g_e^2-2k^2+g_ek)\sin 2\theta}{3\lambda k-3\Delta+\sqrt{(\Delta+3\lambda k)^2+8\Delta^2}}\right]$$

5. Static crystal field consideration, discussion of the results

5.1. The case of the d^1 ion

Two principal components of the g-factor for a d^1 ion as functions of a trigonal field are presented in Fig. 2 at a fixed value of λ ($\lambda = 2000\ cm^{-1}$). The same dependence for the TIP contributions ($\lambda = 2000\ cm^{-1}$) are shown in Fig. 3. Fig. 2a demonstrates that, in the range of negative Δ_{trig}, both $g_\parallel$ and $g_\perp$ are independent of the trigonal field and vanish at $\kappa = 1$. A reduction of κ leads to the increase of $g_\parallel$ due to incomplete compensation of the orbital and spin contributions provided that $\kappa \neq 1$. At the same time, $g_\perp$ remains very small and almost independent of κ as well as Δ_{trig}. An increase in positive Δ_{trig} results in a fast ascent of both g-factors so that, in the range of relatively strong fields, they are close to the spin values of the orbital singlet $^2A_1$. Since in the limit of a strong trigonal field, the spin–orbit interaction is suppressed, the orbital contribution in $^2A_1$ disappears and both g-factors become independent of κ (Fig. 2a and b). The average g-factor is shown in Fig. 3c. In the vicinity of the crossover point $\Delta_{trig} = 0$ (Fig. 1), anomalous non-monotonic behavior of the g-factors versus Δ_{trig} is present.

In the case of $\Delta_{trig} < 0$, the parallel part of the Zeeman interaction does not mix the ground state with the excited ones, and, for this reason, TIP is reduced. Similarly, positive Δ_{trig} increase the gap between the ground and excited states thus reducing the TIP. This leads to the small parallel component of the TIP in both regions of strongly negative and strongly positive Δ_{trig} and the pronounced peak at $\Delta_{trig} = 0$ (Fig. 3a). In contrast to the parallel component, the perpendicular component of the TIP is almost independent of the field at $\Delta_{trig} < 0$ and decreases stepwise at $\Delta_{trig} = 0$ (Fig. 3b). It is remarkable that in the region $\Delta_{trig} < 0$, the constant value of the TIP decreases with the increase of κ. Behavior of the averaged TIP values is shown in Fig. 3c.

5.2. The case of the d^5 ion

Calculated g-factors for fixed $\lambda = -2000\ cm^{-1}$ are shown in Fig. 4 where $\kappa = 1$, $\Delta_{trig} = 0$ and the g-factor is isotropic and purely electronic. It is remarkable that, with the increase of $\Delta_{trig}(\Delta_{trig} < 0)$, the parallel component of the g-factor increases whereas the perpendicular component decreases. In the limit of strong negative Δ_{trig}, $g_\parallel = 4$, $g_\perp = 0$ and $g_{av} = 4/\sqrt{3}$ are obtained. With the increase of Δ_{trig} in the positive direction, the components of the g-factor behave as follows: the parallel component decreases, reaches the minimum, and increases. Both the perpendicular component and the average g-value increase, pass through the maximum and slowly decrease. In the limit of strong positive Δ_{trig}, g-factors again become isotropic and take on the purely electronic value. The decrease of the orbital reduction factor results in the effective decrease of the average g-value. The influence of κ on the different components of g can be observed in Fig. 4.

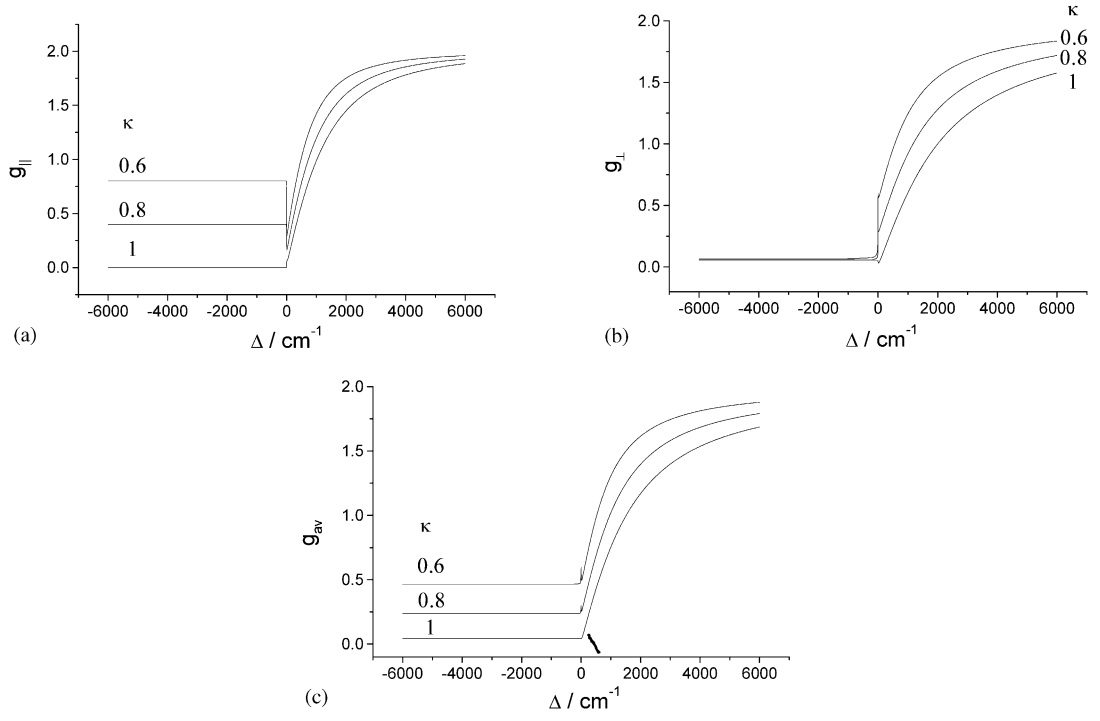

Fig. 2. Calculated g-factors for the trigonally distorted d^1 system as functions of Δ_{trig} and κ.

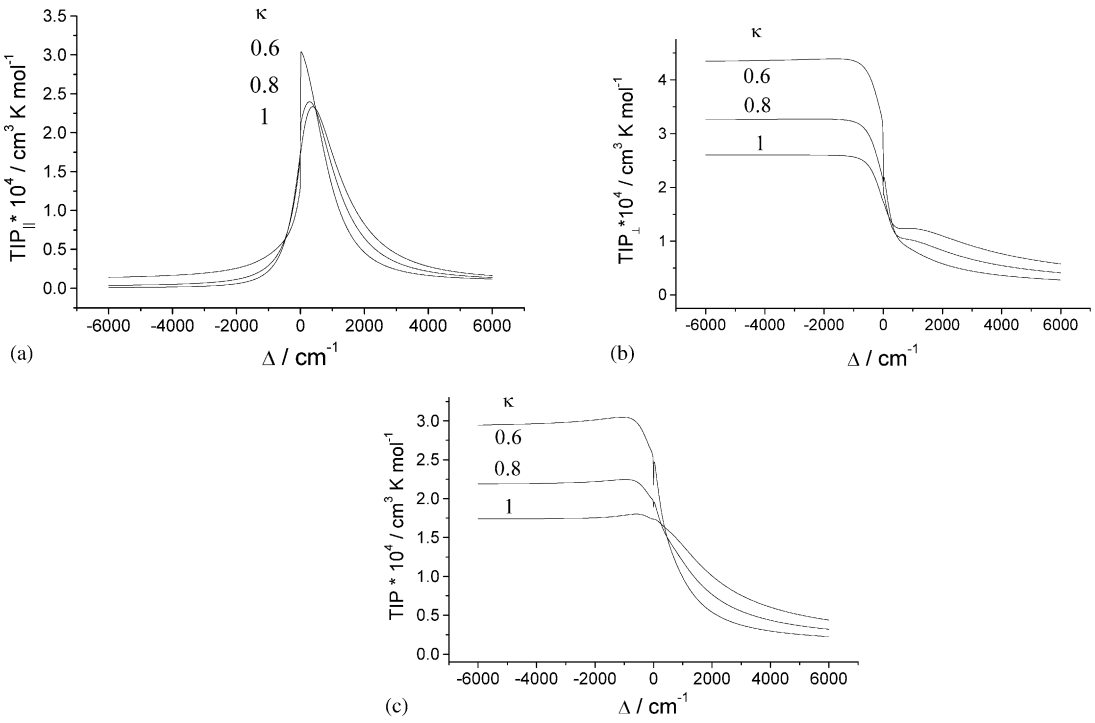

Fig. 3. Calculated TIP contributions for the trigonally distorted d^1 system as functions of Δ_{trig} and κ.

Fig. 5 demonstrates the behavior of TIP for a d^5 system at different values versus κ and Δ_{trig}, assuming fixed $\lambda = -2000$ cm^{-1}. When the external field is applied along the C_3-axis, the TIP has a pronounced maximum at $\Delta_{trig} = 0$ and the value of the TIP at this maximum decreases with the increasing κ (Fig. 5a). In the region of negative field, the TIP is almost independent of the strength of the field and the height of the

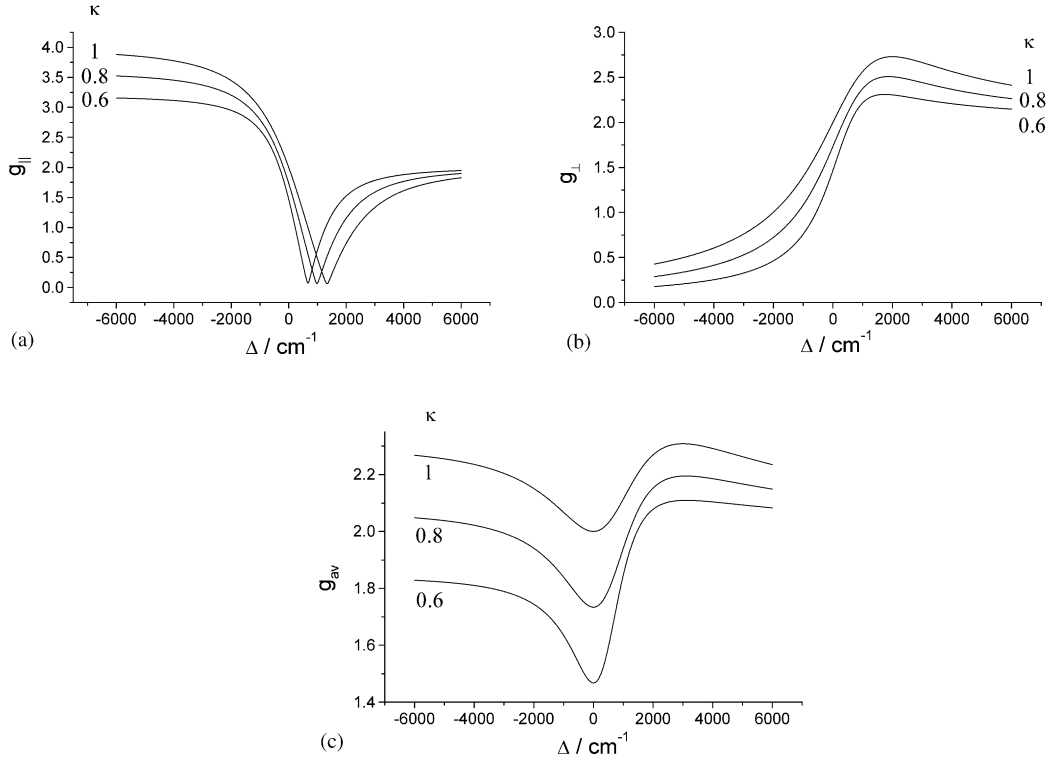

Fig. 4. Calculated g-factors for the trigonally distorted d^5 system as functions of Δ_{trig} and κ.

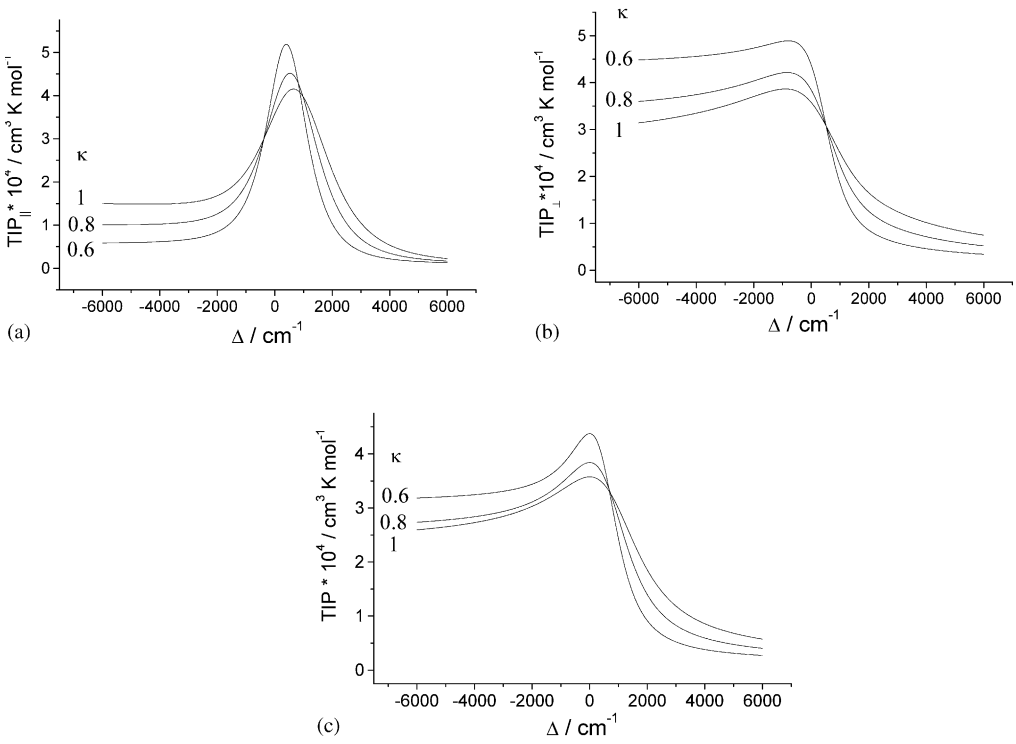

Fig. 5. Calculated TIP contributions for the trigonally distorted d^5 system as functions of Δ_{trig} and κ.

plateau decreases with the decrease of κ. In contrast to the parallel component, the perpendicular TIP component gradually increases in the region of the negative trigonal field, passes through a maximum then decreases rapidly (Fig. 5b). Covalence reduces the perpendicular TIP component in the region of positive trigonal fields while the effect of covalence is of the opposite sign for the negative field. The powder averaged TIP values are shown in Fig. 5c.

6. Pseudo JT problem $^2T_2 \otimes (e+SO)$, magnetic properties

Consideration of the vibronic effects will be restricted to the case of a cubic system ($\Delta_{tetr} = \Delta_{trig} = 0$), and, to simplify the subsequent consideration of the magnetic properties, the main features of the adiabatic surfaces will be discussed assuming that the vibronic interaction with the tetragonal modes is predominant. For a d^1 ion, the ground state is the Γ_8 quadruplet exhibiting first order vibronic effect (JT interaction). This term is mixed with the Γ_6 and leads to an additional pseudo JT interaction, the $(\Gamma_8+\Gamma_6)\oplus$e-problem. The lower sheet possesses three minima located in a circle on the (q_u, q_v) plane at the positions $(q_u, q_v) = (-q_0, 0)$, $(q_0/2, -q_0\sqrt{3}/2)$, $(q_0/2, q_0\sqrt{3}/2)$, where the radius, q_0, of the ring is a function of the spin–orbit parameter, vibronic constant and the frequency ω_e of e-mode (Fig. 6). Each minimum corresponds to the system being

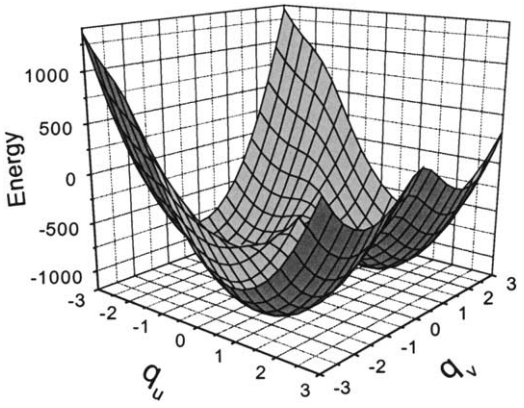

Fig. 6. Lower sheet of the adiabatic surface for $^2T_2 \otimes (e+SO)$-vibronic problem for d^1-ion, $\lambda = 1000$ cm^{-1}, $\hbar\omega = 500$ cm^{-1}, $v = 2\hbar\omega$.

distorted along one of three tetragonal axes. Vibronic effects arise solely from the pseudo Jahn–Teller effect in the case of the d^5 ion. In this case, the landscape of the lower sheet depends on the relative values of the spin–orbit coupling parameter and vibronic constant. If the vibronic interaction is sufficiently weak compared to the spin–orbit coupling, the lower sheet possesses a single minimum at the position (0, 0). This situation is shown in Fig. 7a. With the increase of the vibronic coupling parameter, the cubic configuration becomes unstable, curvature of this adiabatic sheet decreases, and, at a certain value of the vibronic coupling, the single minimum is transformed into three minima (Fig. 7b).

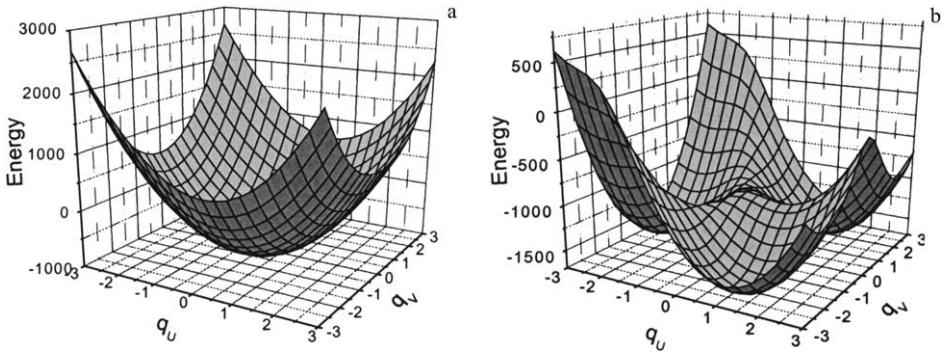

Fig. 7. Lower sheet of the adiabatic surface $^2T_2 \otimes (e+SO)$-vibronic problem for d^5-ion. $\lambda = -1000\ cm^{-1}$, $\hbar\omega = 500\ cm^{-1}$, (a) $\upsilon = 2\hbar\omega$; (b) $\upsilon = 2.5\hbar\omega$.

As in the case of $\lambda > 0$, these minima correspond to the distortions of the system along the tetragonal axes.

In the calculation of the magnetic susceptibility within the adiabatic approach a simplification (based on the assumption that the system is well localized in the vicinity of the minima points of the lower sheet) will be applied so that the corresponding states contribute significantly to the magnetic susceptibility. This simplification allows one to avoid the rather complicated procedure of the integration over the full adiabatic surface in the calculation of the partition function [10], while retaining the main qualitative features of the magnetic behavior over a wide range of parameters. Within this approximation the principal values of the magnetic susceptibility can be computed as follows:

$$\chi_\alpha = NkT\frac{\partial^2}{\partial H_\alpha^2}\left\{\ln\sum_{q\min}\exp[-U_g(q_{\min},\ H_\alpha)/kT]\right\}_{H\alpha\to 0} \tag{19}$$

where $U_g(q_{min}, H_\alpha)$ is the adiabatic energy at the minima (q_{min} is a set of vibronic coordinates supplemented by the Zeeman contribution).

It is important to consider how the vibronic interactions affect the key parameters that determine the magnetic susceptibility, namely the g-factor and the TIP. In each distorted JT configuration, the g-factor and TIP are axially anisotropic. The anisotropy of g-factors can be observed in EPR if the tunneling between the minima is slow enough on the EPR time scale. In the favorable case of slow tunneling, the low-temperature EPR is anisotropic; at higher temperatures the spectrum is transformed into isotropic one [3]. As distinguished from EPR data, the magnetic susceptibility measurements correspond to an 'infinite' time scale of measurement so that the g-factor is averaged over the minima and manifests in the static magnetic characteristics.

Fig. 8a and b show a series of the curves g versus $\upsilon/\hbar\omega$ for a d^1 ion with different values of the orbital reduction factor κ. In the case of weak vibronic coupling, both components of g are small, which conforms to the crystal field consideration. The JT interaction is active in the ground state quadruplet and localization of the system in the minima of the adiabatic potential gives rise to an effective tetragonal deformation. An increase of the vibronic coupling leads to the increase of g-factors due to pseudo JT mixing of the low-lying Γ_8 with the excited doublet Γ_6. In the limit of strong vibronic coupling when spin–orbit coupling is eliminated, the ground state becomes (according to the Jahn–Teller theorem) the orbital singlet. Combined JT and pseudo JT interaction suppresses spin–orbit coupling so that the orbital singlet exhibits a pure electronic g-factor. When $\kappa \neq 0$, the Γ_8 quadruplet becomes

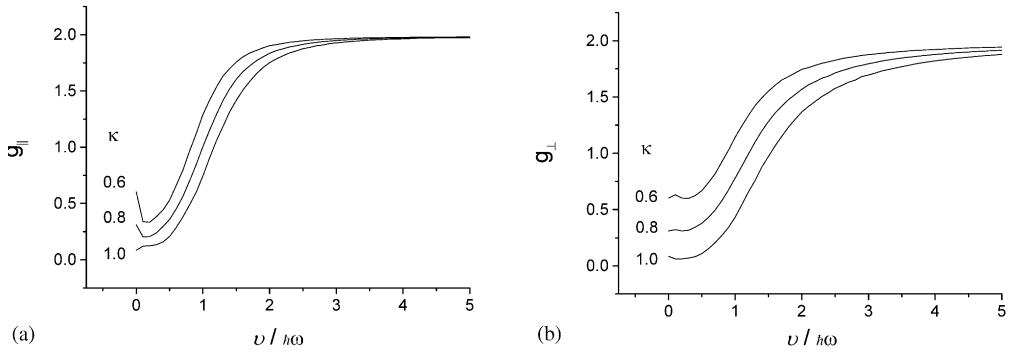

Fig. 8. Calculated values of the g-factors for the d^1 ion as functions of the vibronic parameter in $^2T_2 \otimes (e+SO)$-vibronic problem. $\lambda = 1000\ cm^{-1}$, $\hbar\omega = 500\ cm^{-1}$.

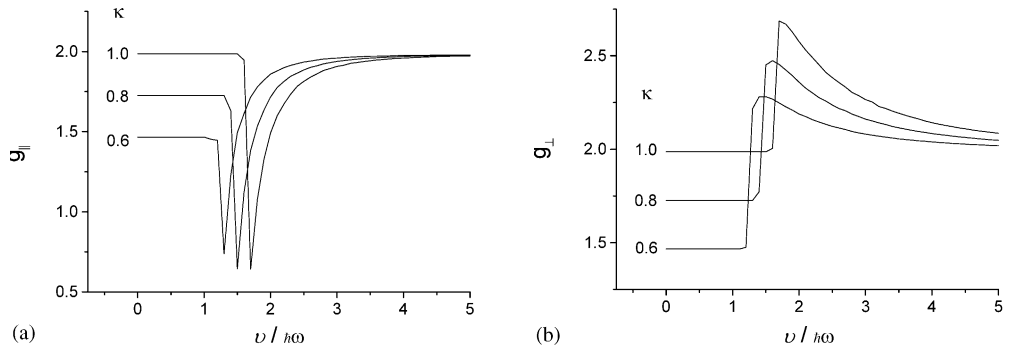

Fig. 9. Calculated values of the g-factors for the d^5 ion as the functions of the vibronic parameter in $^2T_2 \otimes (e+SO)$-vibronic problem. $\lambda = -1000$ cm^{-1}, $\hbar\omega = 500$ cm^{-1}.

magnetic so that g increases with the decrease of κ. This effect is more pronounced when the vibronic interaction is weak and it vanishes in the limit of strong vibronic coupling because of complete localization in the minima and suppression of spin–orbit coupling.

Fig. 9 shows the principal values of the g-factors for a d^5 ion as functions of the vibronic coupling parameter, for different values of the reduction factor. In this case the ground electronic state ($\upsilon/\hbar\omega = 0$) is Γ_7, so the g-factor is maximal providing $\kappa = 1$ ($g = 2$) and decreases with decreasing κ. In the range of relatively small υ that do not exceed some critical value υ_c, both curves $g_{\parallel}$ and $g_{\perp}$ versus $\upsilon/\hbar\omega$ exhibit plateaus. At $\upsilon < \upsilon_c$ $g_{\parallel}$ has a deep minimum then reaches a saturation value $g_{\parallel} = 2$ that is independent of κ. The position of the minimum moves in the region of larger υ with the increase of κ. At $\upsilon > \upsilon_c$, $g_{\perp}$ increases stepwise with the increase of υ, goes through a maximum and then gradually decreases up to a value of 2 that is common for all κ. The plateau in the dependences $g_{\parallel}$ and $g_{\perp}$ versus $\upsilon/\hbar\omega$ appear due to the fact that for small vibronic coupling $\upsilon < \upsilon_c$, the lower sheet of the adiabatic surface has the only minimum corresponding to the high-symmetric nuclear configuration. Each plateau ends at the value of $\upsilon = \upsilon_c$ corresponding to the condition of instability for which a single-minimum surface is transformed into the surface possessing three tetragonal minima (see Fig. 7). The vibronic mixing of the electronic states in these minima leads to a sharp minimum in $g_{\parallel}$ and to the increase of $g_{\perp}$ within a relatively narrow region of vibronic parameters followed by a slow decrease. A decrease of κ lowers the gap between Γ_6 and Γ_8 that favors pseudo JT instability, which accounts for the dependence of υ_c upon κ in Fig. 9. In the limit of strong vibronic coupling, the pure electronic g-factor is attained. This behavior is compatible with the dependences of g-factors on the strength of static trigonal crystal field (Fig. 4). Fig. 10 illustrates how the above-mentioned features of the principal components of g-factors manifest themselves in the behavior of the average values.

The TIP contributions as functions of $\upsilon/\hbar\omega$ for d^1 and d^5 ions are shown in Fig. 11a and b respectively. In both cases the vibronic interaction produces similar effects on the TIP. The main common feature of the curves in Fig. 11a and b is the decrease of the TIP with the increase of vibronic coupling. This is obviously the result of JT splitting that increases the energy gap between the minima of the lower adiabatic surface sheet and the energy of the upper sheet in this nuclear configuration. This leads to the vibronic reduction of the second order

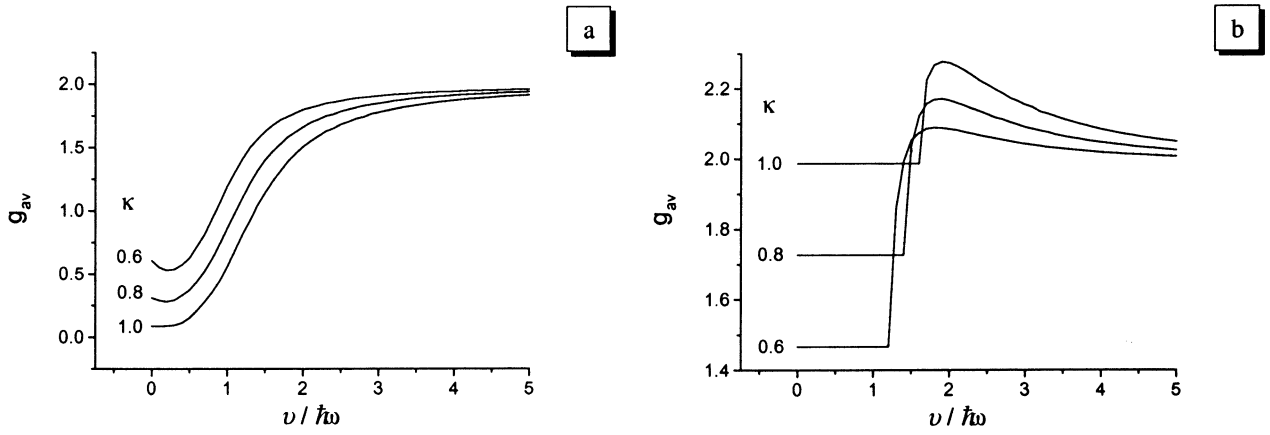

Fig. 10. Calculated dependence of the powder averaged g vs. $\upsilon/\hbar\omega$ values in $^2T_2 \otimes (e+SO)$-vibronic problem: (a) d^1-ion. $\lambda = 1000$ cm^{-1}, $\hbar\omega = 500$ cm^{-1}; (b) d^5-ion, $\lambda = -1000$ cm^{-1}, $\hbar\omega = 500$ cm^{-1}.

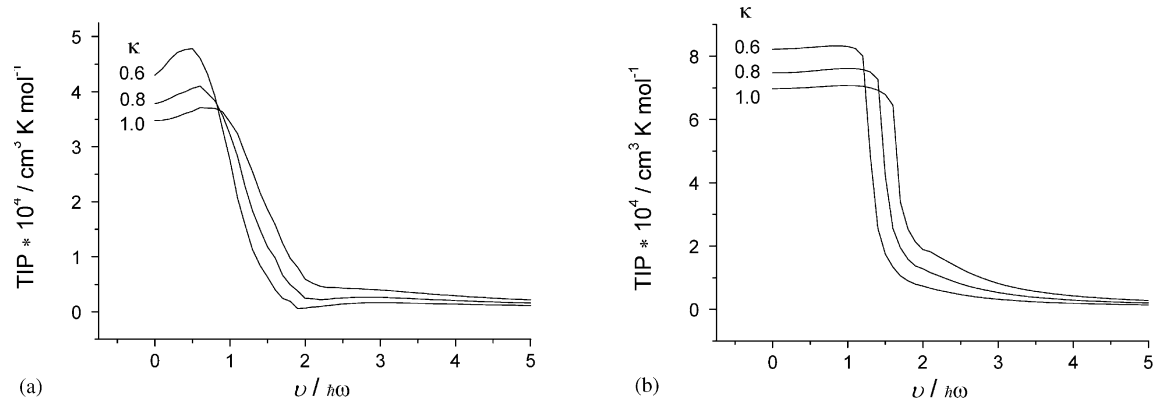

Fig. 11. TIP vs. $\upsilon/\hbar\omega$ curves in $^2T_2 \otimes (e+SO)$-vibronic problem: (a) d^1-ion, $\lambda = 1000\ cm^{-1}$, $\hbar\omega = 500\ cm^{-1}$; (b) d^5-ion, $\lambda = -1000\ cm^{-1}$, $\hbar\omega = 500\ cm^{-1}$.

Zeeman effect that is responsible for the TIP. Regarding the influence of the orbital reduction factor on the TIP, it can be noted that for small $\upsilon/\hbar\omega$, TIP increases with the decrease of κ. It can be surmised that this decrease arises from the fact that for $\upsilon/\hbar\omega = 0$ the energy separation between the ground and excited spin–orbit multiplets is proportional to κ. Accordingly, for larger κ the TIP is reduced. With the increase of vibronic coupling the vibronic reduction of spin–orbit interactions also begin to play an important role. This reduction is more pronounced when the effective spin–orbit interaction is weaker, or, when κ is smaller. This accounts for, at a certain value of $\upsilon/\hbar\omega$, the order of the curves changing in such a way that the larger TIP corresponds to the larger value of κ.

It should be noted that, in the vicinity of the point of nuclear instability, the adiabatic approximation fails due to strong dynamic coupling between electronic and nuclear motion. Precise description of g-factors and TIP in this region should be based on dynamic vibronic calculations and take into account for the kinetic energy of the ions.

The described behavior of g-factors and TIP contributions are manifested in the averaged χT versus T dependency plots shown in Fig. 12a for a d^1 ion and in Fig. 12b for a d^5 ion. The low temperature limit of χT is proportional to g^2, while the slope of the χT versus T lines are directly related to the TIP. One can see that for the d^1 ion, the increase of vibronic coupling leads to an increase of χT and a decrease of the slope. This behavior is quite compatible with the already discussed dependencies of g versus T and TIP versus T. The same is true for the case of the d^5 ion where the low-temperature χT value and the slope non-monotonically depend on the vibronic parameter (as opposed to the behavior of the g-factor and TIP). An essential difference between the low-symmetry field and JT (pseudo JT) distortions must be noted. In the former case both signs of the distortions and consequently both ground states ($^2A_1$ and ^2E) are physically meaningful. In contrast, in accordance with the JT theorem, the minima points of the adiabatic potential correspond to the orbitally singlet ground state.

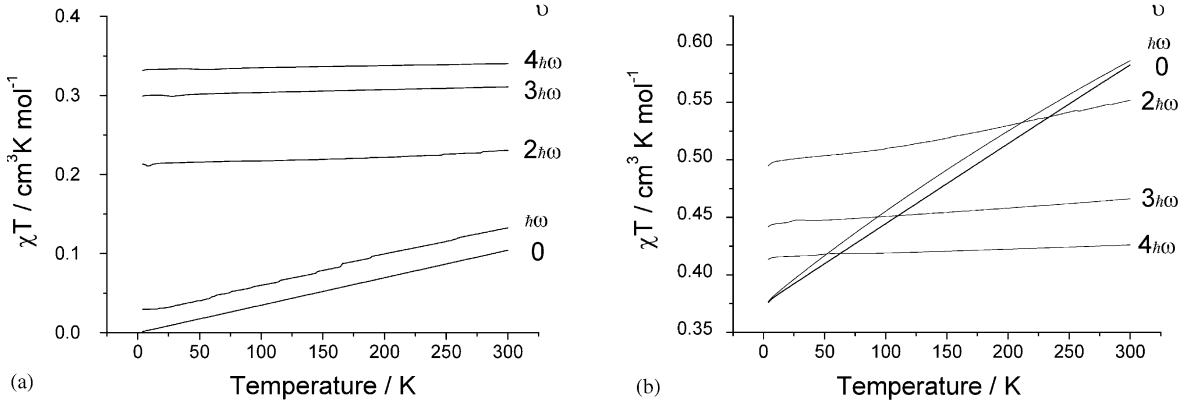

Fig. 12. χT vs. T curves for $\kappa = 1$ in $^2T_2 \otimes (e+SO)$-vibronic problem: (a) d^1-ion, $\lambda = 1000\ cm^{-1}$, $\hbar\omega = 500\ cm^{-1}$. (b) $\lambda = -1000\ cm^{-1}$, $\hbar\omega = 500\ cm^{-1}$.

7. Concluding remarks

In this work, the magnetic behavior of d^1 and low-spin d^5 ions possessing well-isolated $^2T_2$ ground states have been investigated. The model takes into account a strong cubic crystal field, spin–orbit coupling within a $^2T_2$ term, low symmetry crystal fields and vibronic JT and pseudo JT interactions. It was shown that the magnetic properties of these systems strongly depend on all these interactions. Axial distortions that stabilize orbital doublets result in strongly anisotropic g-factor and TIP contributions. Distortions of the opposite sign (that stabilize the singlet) decrease the anisotropy of g so that, in the limit of strong distortions, we arrive to a purely electronic, isotropic g-value accompanied by a vanishing TIP value. It should also be mentioned that for all sets of parameters, the maximal value of TIP corresponds to the symmetric system.

In the framework of the semi-classic adiabatic approximation we have also analyzed the influence of the vibronic effects in the relatively simple case of a cubic system. For the sake of simplicity only the interaction of the electronic shell with the tetragonal vibrational modes has been taken into account. JT distortions produce effects that are similar to those arising from the static crystal field that stabilizes the orbital singlet. The vibronic effects are critically different for d^1 and d^5 ions. In the former case, the ground state quadruplet Γ_8 is JT active, while for the d^5 ion, only pseudo JT effects result in the instability of the system. This leads to a specific behavior of the magnetic characteristics as functions of the vibronic parameter. The low-temperature limit of χT versus vibronic parameter for the d^1 ion increases with the increase of the vibronic coupling concomitant with a strongly decreasing TIP. The low temperature limit of χT for d^5 ions behaves non-monotonically. An increase of the vibronic coupling leads to an increase of this value, then a sharp decrease. TIP decreases with the increase of vibronic coupling. Regarding the vibronic JT problem, it should be noted that the adiabatic approximation works well if the vibronic coupling strong enough. In this case the minima of the adiabatic potential are deep so that the system is well localized. In the case of moderate vibronic coupling when the depth of the minima is comparable with $\hbar\omega$, this adiabatic approximation fails and the system should be described by vibronic (hybrid) functions. As was shown in [4] this circumstance leads to the essentially new magnetic behavior of a d^1 system possessing a JT ground state Γ_8. In this view one can expect that the pseudo JT effect in d^5 ions can give rise to a similar behavior in the range of intermediate vibronic coupling. We are poised to consider this question elsewhere and to apply the presented theory to the named Re(II) compounds.

Acknowledgements

Financial support of US Civilian Research and development Foundation, CRDF (Award MP2-3022), National Science Foundation Nanoscale Science and Engineering NIRT Grant (DMR-0103455), National Science Foundation PI-Grant (NSF CHE-9906583), and the Supreme Council on Science and Technological Development of Moldova (grant 111) is highly appreciated.

References

[1] J. Schelter, J.K. Bera, J. Bacsa, J.R. Galán-Mascarós, K.R. Dunbar, Inorg. Chem. (2002) submitted.
[2] B. Bleaney, M.C.M. O'Brien, Proc. Phys. Soc. B69 (1956) 1216.
[3] A. Abragam, B. Bleaney, Electron Paramagnetic Resonance of Transition Ions, Clarendon Press, Oxford, 1970.
[4] A.C. Chakravarty, Introduction to the Magnetic Properties of Solids, Wiley, NY, 1980.
[5] S.A. Al'tshuler, B.M. Kozirev, Electron Paramagnetic Resonance, Nauka, Moskva, 1972.
[6] R. Englman, The Jahn–Teller Effect in Molecules and Crystals, Wiley, London, 1972.
[7] I.B. Bersuker, The Jahn–Teller Effect and Vibronic Interactions in Modern Chemistry, Plenum, NY, 1984; Chem. Rev. 101 (2001) 1067.
[8] I.B. Bersuker, V.Z. Polinger, Vibronic Interaction in Molecules and Crystals, Springer, NY, 1989.
[9] P.L.W. Tregenna-Piggot, M.C.M. O'Brien, H. Weiche, H.U. Güdel, J. Chem. Phys. 109 (1998) 2967.
[10] J.J. Borrás-Almenar, E. Coronado, H.M. Kishinevsky, B.S. Tsukerblat, Chem. Phys. Lett. 217 (1994) 525.
[11] J.J. Borrás-Almenar, J.M. Clemente-Juan, E. Coronado, A.V. Palii, B.S. Tsukerblat, Chem. Phys. 274 (2001) 131; 274 (2001) 145.
[12] D.A. Varshalovich, A.N. Moskalev, V.K. Khersonskii, Quantum Theory of Angular Momentum, World Scientific, Singapore, 1988.
[13] O. Kahn, Molecular Magnetism, VCH Publishers, New York, 1993.